scientific reports

Check for updates

OPEN

Bacillus-mediated transcriptional and metabolic reprogramming elicits defense priming in *Coptis chinensis* roots

Na Li[1,3], Hailang Liao[2], Chi Zhang[1,3], Feifei Xu[1,3], WenJia Ke[1,3], Yang Xiao[1,3], JiJing Dong[5], BinJie Xu[4]✉, Tao Zhou[1,3]✉ & YunTong Ma[1,3]✉

The medicinal plant *Coptis chinensis* is highly susceptible to root rot caused predominantly by *Fusarium* spp., threatening yield and medicinal quality. Biological control agents (BCAs) from the genus *Bacillus* are promising, yet their host mechanisms remain incompletely defined. We evaluated a four-strain *Bacillus* consortium as BCAs in field-grown *C. chinensis* and profiled host roots using transcriptomics and metabolomics. Pre-inoculation with the BCA mixture resulted in a modest, albeit statistically non-significant, reduction in disease index following *Fusarium solani* challenge. Multi-omics analyses showed that BCA treatment reprogrammed genes and metabolites associated with amino acid metabolism, accompanied by increased glutamine (Gln) accumulation. Supplementing culture medium with exogenous Gln inhibited *F. solani* growth in a concentration-dependent manner in vitro. Notably, *F. solani* or BCAs alone elicited modest regulation of canonical defense genes, whereas BCA pre-inoculation followed by *F. solani* robustly up-regulated defense modules across MAPK signaling, plant–pathogen interaction, and hormone signaling (JA, ET, SA), consistent with molecular immune priming. These results suggest that the BCA consortium induces resistance- and priming-related molecular markers in *C. chinensis* by modulating amino acid metabolism and host immunity. These findings provide a mechanistic basis for the potential application of BCAs in the sustainable management of *C. chinensis* root rot.

Keywords *Coptis chinensis*, *Bacillus*, *Fusarium* root rot, Nitrogen assimilation, Priming

Rhizoma Coptidis (RC), the rhizome of the perennial medicinal herb *C. chinensis*, has been used for millennia in traditional Chinese medicine for heat-clearing, dampness-drying, and detoxification, and is a key component of classic formulae such as Huanglian Tang, Huanglian Jiedu Tang, and Huanglian Ejiao Tang[1,2]. Modern pharmacology attributes broad activities to RC including antibacterial, antiviral, cardioprotective, anticancer, and potential anti-diabetic and anti-Alzheimer's effects[3,4]. RC is widely used in East Asian (China, Japan, Korea, Malaysia, and Singapore)[5], with an annual demand of 3,500–4,000 tons that continues to rise[6]. China supplies roughly two-thirds of global output, approximately 90% of which comes from cultivation, with major production centers in Shizhu County (Chongqing) and Lichuan City (Hubei)[7]. As cultivation expands and fields are continuously cropped, disease pressure has intensified. Root rot is among the most severe problems, with reported incidence in Shizhu of ~40% and yield losses approaching 67%[8].

Root rot is a globally prevalent soil-borne disease that severely affects the growth and development of many plant species[9]. In China, since first reports in 1989, its distribution has expanded to Xinjiang, Gansu, Heilongjiang, Jilin, Guizhou, and Sichuan[10]. Losses can be substantial, for example, 5–20% annually in *Panax notoginseng* (reaching 70% or complete crop failure in severe cases) and 30–90% in cultivated American ginseng[11,12]. Typical symptoms include root browning and decay, stunting, leaf chlorosis and wilting, and plant death[9]. Although

[1]State Key Laboratory of Southwestern Chinese Medicine Resources, Chengdu University of Traditional Chinese Medicine, Chengdu 611137, Sichuan, China. [2]Industrial Crop Research Institute, Sichuan Academy of Agricultural Sciences, Chengdu 610300, Sichuan, China. [3]College of Pharmacy, Chengdu University of Traditional Chinese Medicine, Chengdu 611137, Sichuan, China. [4]Innovative Institute of Chinese Medicine and Pharmacy, Chengdu University of Traditional Chinese Medicine, Chengdu 611137, Sichuan, China. [5]Traditional Chinese Medicine Hospital of Ya'an, Ya'an, Sichuan, China. ✉email: binjiexu@outlook.com; 364462907@qq.com; mayuntong@cdutcm.edu.cn

bacteria and nematodes can contribute, fungi—especially *Fusarium* spp.—are recognized as principal causal agents across many medicinal plants, including *R. glutinosa*, *A. sinensis*, and *C. chinensis*[10].

Integrated management—combining precision field hygiene, judicious fungicide use, and biological control—offers the most practical approach because above-ground symptoms often appear late[9]. Microbial biocontrol has shown particularly promising efficacy and translational potential[13]. For example, strains isolated from *Angelica* rhizosphere (YF, SY89) produce IAA and siderophores, promote root growth, and reduce disease indices by more than 60%[14]. In addition, *Trichoderma harzianum*, *Pseudomonas putida*, *Bacillus pumilus*, and *Burkholderia cenocepaciaand* have been successfully used to suppress root rot in pea, maize, and other crops[15,16].

Biocontrol agents mitigate disease via direct pathogen suppression and/or enhancement of plant resistance. Beneficial microbes can rapidly colonize plant surfaces, tissues, and the rhizosphere, occupying ecological niches and competing with pathogens for nutrients[17]. Many produce antibiotics, cell-wall-degrading enzymes, and other metabolites that directly inhibit pathogens[18,19]. Exposure to non-pathogenic microbes may triggers defense responses, particularly during the early stages of interaction[20,21]. Microbes can also elicit the accumulation of defensive metabolites (e.g., phenolics, alkaloids, and flavonoids)[22,23]. Increasingly, primary metabolites are recognized as important in plant defense[24]. For example, galactitol accumulates during pathogen infection and contributes to systemically induced resistance[25], threonine functions as a signaling molecule in *Arabidopsis* defense[26], and glutamate (Glu)—a principal amino-group donor for nucleotide and nitrogen-containing compound biosynthesis—has been implicated as a defense-related signal[27].

Previously, we profiled the rhizosphere and endophytic microbiomes of healthy versus diseased *C. chinensis* plants and observed a negative correlation between *Bacillus* and pathogenic *Fusarium*. Notably, four *Bacillus* strains isolated from healthy *C. chinensis* displayed pronounced antagonism against root rot pathogens including *F. solani* and *F. avenaceum*[28]. Whether these *Bacillus* strains effectively reduce root rot under field conditions, and by what mechanisms, remains unclear. Here, we assess their efficacy in preventing or ameliorating root rot and examine host transcriptomic and metabolomic responses to elucidate the underlying mechanisms.

Materials and methods

In vitro compatibility among four *Bacillus* strains

Four antagonistic strains—*B. mycoides* GJ-LB-021, *B. pseudomycoides* GJ-YEM-005, *B. velezensis* GJ-JM-1, and *B. subtilis* GJ-TR-064—were assayed pairwise on nutrient agar (NA) base plates (10 mL per plate). For each strain, 500 µL of an overnight culture was mixed with 10 mL semi-solid NA, gently swirled, and overlaid to form the indicator lawn[29]. The test strain (3–4 µL overnight culture) was spot-inoculated at the center; assays were performed reciprocally for each pair. Plates were incubated at 37 °C for 24 h and inspected. Compatibility was inferred from the presence or absence of a clear inhibition zone around the central colony.

Microbial strains and culture conditions

Preparation of F. solani spore suspension

F. solani (isolated and identified in a previous study[28] was inoculated onto potato dextrose agar (PDA) plates and incubated in darkness for 3 days. A single colony was then transferred to potato dextrose broth (PDB) and cultured at 25 °C with shaking at 120 rpm for 4 days. The resulting culture was filtered through four layers of lens paper to obtain a clarified filtrate. Spores were collected by centrifugation at 6,000 rpm for 3 min, washed twice with sterile sterile PBS buffer to remove residual impurities, and resuspended in sterile PBS to 1×10^7 cfu/mL.

Preparation of the biological control agents (BCAs)

Single colonies of each *Bacillus* strain were grown in NA broth at 37 °C, 120 rpm for 24 h. Cells were harvested (6,000 rpm), washed twice with sterile PBS, and resuspended in sterile PBS. The suspension was adjusted to OD_{600}= 1.0 (corresponding to approximately 1×10^9 cfu/mL for each strain). The four strains were then mixed in equal volumes.

Field site, design, and sampling

The experimental plants were one-year post-transplantation *C. chinensis* (preceded by a two-year seedling nursery period) at the new root emergence stage (voucher specimen deposited in the Artificial Climate Chamber of Chengdu University of Traditional Chinese Medicine, identified by Prof. Yuntong Ma, voucher No. WWS-GP-240608-001), supplied by Wa'wu Mountain Pharmaceutical Co., Ltd. The field trials were conducted at the company's *Coptis* cultivation base in Group 2, Heshan Village, Gaomiao Town, Hongya County, Meishan City, Sichuan Province, China (29°29′10.91″ N, 103°9′39.9″ E). The soil at this site is a typical yellow-brown soil with a slightly acidic pH, representative of the primary *C. chinensis* producing regions. To minimize the confounding effects of continuous cropping obstacles—such as soil degradation, autotoxicity, and pre-existing pathogen accumulation common in older *Coptis* fields[30]—this study was specifically performed on a newly cultivated plot with no prior history of *C. chinensis* planting. A pre-experimental survey confirmed the absence of root rot symptoms in the selected area, providing a healthy and standardized baseline for the subsequent *Fusarium* challenge. The area was partitioned into 12 plots in a 4 × 3 grid, each containing about 180–200 healthy plants (Supplementary Fig. S1). Four treatments were applied: (1) sterile PBS control (CK); (2) *F. solani* only (Fs); (3) BCAs only (BCA); (4) BCA pre-inoculation followed 7 d later by *F. solani* (BCAFs). With appropriate modifications based on the protocol described by Marsell and Fröschel[31], a surface drip irrigation-based method was employed for inoculum delivery. Specifically, 10 mL of the inoculum was directly injected into the soil surrounding each plant using a sterile syringe. To maintain consistency in the duration of pathogen exposure, the disease index (DI) was assessed 7 days post-inoculation (dpi) with *F. solani*. Specifically, DI was recorded at day 7 for the Fs group and at day 14 for the BCAFs group. For the control groups (CK and BCA), DI was

recorded at the end of the experiment (day 14) to confirm the absence of disease symptoms. Fifteen plants per treatment were scored; five plants per treatment were sampled for root transcriptomics and metabolomics.

Disease index assessment

Following published methods[32], 15 plants per treatment were scored on a six-point scale (0–5):

Grade 0: Rhizomes and fibrous roots intact; no visible lesions; no leaf wilting.
Grade 1: Scattered lesions confined to fibrous roots; trace infection; no leaf wilting.
Grade 2: ≤25% of fibrous roots infected (mild); no leaf wilting.
Grade 3: >25% to ≤ 50% of fibrous roots infected; no leaf wilting.
Grade 4: >50% to ≤ 75% of fibrous roots infected, with leaf wilting in ≤ 25% of leaves.
Grade 5: >75% of fibrous roots infected, rhizomes rotted, with ≥ 50% of leaves wilted.
The disease index was calculated using the following formula:

$$\text{Disease Index} = \frac{\sum \text{grade} \times \text{Number of plants of that grade}}{5 \times \text{Total Number of plants}} \times 100\% \quad (1)$$

Metabolomic analysis of *C. chinensis* roots

Metabolites were extracted, identified and quantified by Wekemo Tech Group Co., Ltd. (Shenzhen, China) with five biological replicates per treatment using LC–MS/MS system (Ultra-High Performance Liquid Chromatography, Thermo Vanquish; Mass Spectrometer, Thermo Q Exactive series). The LC and MS conditions, as well as the qualitative and quantitative analyses of metabolites, were set as described by Cao et al.[33]. Principal component analysis (PCA) and orthogonal partial least-squares discriminant analysis (OPLS-DA) were performed to assess global metabolic variations among samples. Differentially accumulated metabolites (DAMs) were selected using the criteria variable importance in projection (VIP) ≥ 1, FDR < 0.05 and fold change (|FC|) ≥ 1.2.

Transcriptomic analysis of *C. chinensis* roots

RNA-seq (Illumina HiSeq) was performed by Wekemo Tech Group Co., Ltd. (Shenzhen, China) on four groups with five biological replicates each. The downstream analyses were performed through the company's online pipeline[34]: (1) adapters and low-quality bases were trimmed with fastp (v0.21.3) to obtain clean data; (2) clean reads were mapped to the *C. chinensis* reference genome JADFTS000000000.1 (https://www.ncbi.nlm.nih.gov/nuccore/1936226600) using HISAT2 (v2.2.0)[35,36]. Only uniquely mapped reads (aligned once) were retained for subsequent analyses; (3) gene-level read counts were quantified with featureCounts (v2.0.1) and normalized to fragments per kilobase of transcript per million mapped reads (FPKM)[37]; (4) differentially expressed genes (DEGs) were identified with DESeq2 (v1.26.0) using |FC|≥1.2 and FDR < 0.05[38] ; (5) kyoto encyclopedia of genes and genomes (KEGG) was used to analyze pathways mainly involved in the DEGs[39,40]. All KEGG pathway maps used in this study were obtained from the KEGG database (www.kegg.jp/kegg/kegg1.html).

The detection of quantitative real-time PCR (qRT-PCR)

Total RNA was extracted from *C. chinensis* roots using a plant RNA extraction kit (Takara Biomedical Technology, Beijing Co., Ltd.) following the manufacturer's instructions. First-strand cDNA was synthesized with HiScript II Q RT SuperMix (Beijing Qingkai Biotechnology Co., Ltd.). RT-qPCR was performed in 2×RealStar Green Fast Mix (BioRad, Shanghai, China) on a CFX96 Touch Real-Time PCR System (Thermo Fisher Scientific). The *C. chinensis* 18 S gene was used as an internal reference for normalization. Gene-specific primers (Supplementary Table S1) were designed using Primer 5.0, and relative expression levels were calculated using the $2^{-\Delta\Delta Ct}$ method.

Effects of L-Glutamine on the growth of *F. solani*

Following the method described by Chen, H. F. et al.[41], L-Glutamine (L-Gln) stock was added to PDA cooled to approximately 60℃, to yield final concentrations of 1.0, 2.0, 3.0, 5.0, and 8.0 mmol/L. Mycelial plugs (8 mm diameter) were cut from the actively growing margin of 7-day *F. solani* cultures and placed on the amended PDA plates and incubated at 28℃. Colony diameters were measured at 3 and 7 days. PDA without L-Gln served as control.

Statistical analysis

All statistical analyses were conducted using IBM SPSS Statistics 27.0 (IBM Corp., Armonk, NY, USA). Quantitative data are expressed as the mean ± standard deviation (SD). For the disease index (DI) assessment, 15 independent plants were evaluated per treatment group ($n = 15$), and significant differences were determined using the Kruskal-Wallis test. For the qPCR analysis and the in vitro L-Glutamine inhibitory assays, three ($n = 3$) and five ($n = 5$) independent biological replicates were employed, respectively. Data normality and homogeneity of variance were confirmed prior to analysis. Differences among groups were analyzed using one-way analysis of variance (ANOVA) followed by Tukey's post-hoc test. Statistical significance was defined as $P < 0.05$.

Results

Bacillus strains partially attenuate *C. chinensis* root rot in the field

The four *Bacillus* isolates showed no mutual growth inhibition in vitro (Supplementary Fig. S2), supporting their use as a mixed inoculum. In field trials, above-ground tissues exhibited no visible symptoms across treatments, whereas *F. solani*-inoculated roots displayed browning and decay (Fig. 1). *F. solani* alone caused mild disease (DI = 6.67%; Supplementary Table S2), while BCAs alone caused none. Notably, pre-inoculation with BCAs followed by *F. solani* reduced DI to 4.00%, although this reduction was not statistically significant ($P > 0.05$).

Fig. 1. Preventive efficacy of BCAs against *C. chinensis* root rot caused by *F. solani*. (**A**) Control plants treated with sterile PBS for 14 days. (**B**) Inoculated with *F. solani* (Fs) for 7 days. (**C**) Treated with biocontrol agents (BCAs) for 14 days. (**D**) Pre-inoculated with BCAs for 7 days, then challenged with *F. solani* for 7 days.

Metabolomic profiles associated with BCA-mitigated *C. chinensis* root rot

Across treatments, 533 metabolites spanning 13 classes were detected; lipids (18.6%), flavonoids (11.1%), terpenoids (10.7%), carbohydrates and derivatives (9.8%), and organic acids (9.4%) predominated (Fig. 2A). Principal-component analysis (PCA) clearly separated the four treatments (Fig. 2B), with PC1 and PC2 jointly explaining 30.56% of the total variance. Relative to CK group, *F. solani* infection increased 18 metabolites (Fig. 2C, D), notably lipids (e.g., LPA 18:2, LPI 18:3, 9-HpOTrE) and carbohydrates (e.g., D-gossypose, trehalose, stachyose). BCAs treatment elevated 23 metabolites (Fig. 2C, E), including amino acids/derivatives (L-Gln, 5-oxoproline, D-phenylalanine), sugars, and lipids (e.g., 13(S)-HOTE, 9-HpODE, 9-HpOTrE, methyl jasmonate), while decreasing certain phenolic acids (e.g., 5-*O*-caffeoylshikimic acid). Compared with Fs group, BCAFs further increased L-Gln, 5-oxoproline, D-(-)-Lyxose, and N-Acetylglucosamine, while decreasing lipids such as LPA 18:2, arachidonic acid, and eleostearic acid (Fig. 2F).

Transcriptomic reprogramming underlies BCAs effects

To further elucidate how biocontrol agents alleviate *C. chinensis* root rot, we performed transcriptome profiling. In total, 20 cDNA libraries were constructed, yielding 40,401,024–74,075,838 clean reads per library (Supplementary Table S3). Q20 and Q30 exceeded 97.29% and 91.51%, respectively, and the GC content ranged from 41.08% to 42.50% (Supplementary Table S3). PCA clearly separated roots transcriptomes by microbial treatment, with PC1 and PC2 explaining 23.5% and 11.06% of the variance, respectively (Supplementary Fig. S3). Differential expression analysis revealed that *F. solani* triggered 469 up-regulated and 277 down-regulated genes (Fig. 3A, Supplementary Table S4). Notably, pre-inoculation with BCAs followed by *F. solani* (BCAFs) yielded 1,887 up-regulated and 1,279 down-regulated genes (Fig. 3E, Supplementary Table S4), indicating robust transcriptional reprogramming upon sequential exposure to beneficial and pathogenic microbes.

KEGG pathway enrichment analysis revealed that *F. solani* infection predominantly affected the ribosome, flavonoid/flavonol biosynthesis, and fatty-acid biosynthesis/metabolism (Fig. 3B, Supplementary Table S5). In contrast, BCAs enriched monoterpenoid biosynthesis, motor proteins, arginine biosynthesis, and valine/leucine/isoleucine degradation (Fig. 3D, Supplementary Table S5). Relative to the Fs group, BCAFs further enriched terpenoid biosynthesis, alanine/aspartate/glutamate metabolism, valine/leucine/isoleucine degradation, MAPK signaling, and plant-hormone signaling (Fig. 3F, Supplementary Table S5).

We next examined DEGs involved in nitrogen and amino acid metabolism. In the BCA group, genes associated with nitrogen assimilation and Glu metabolism were markedly enriched (Fig. 4A), including *NRT2*, *NR*, *NiR*, and *GDH*, which facilitate primary nitrogen assimilation and Gln synthesis—consistent with the observed Gln accumulation. Following sequential BCA pre-inoculation and subsequent *F. solani* challenge, nitrogen-assimilation genes were down-regulated, whereas *GLU*- and *GAD*-annotated genes (involved in Glu and γ-aminobutyric acid metabolism) were up-regulated, indicating pronounced modulation of N and amino-acid metabolism under sequential inoculations. The qRT-PCR corroborated these trends, showing significantly elevated *NRT2*, *NiR*, and *GDH* transcripts under BCA treatment, whereas *GAD* and *GLU* transcripts were highest in the BCAFs group (Fig. 4B).

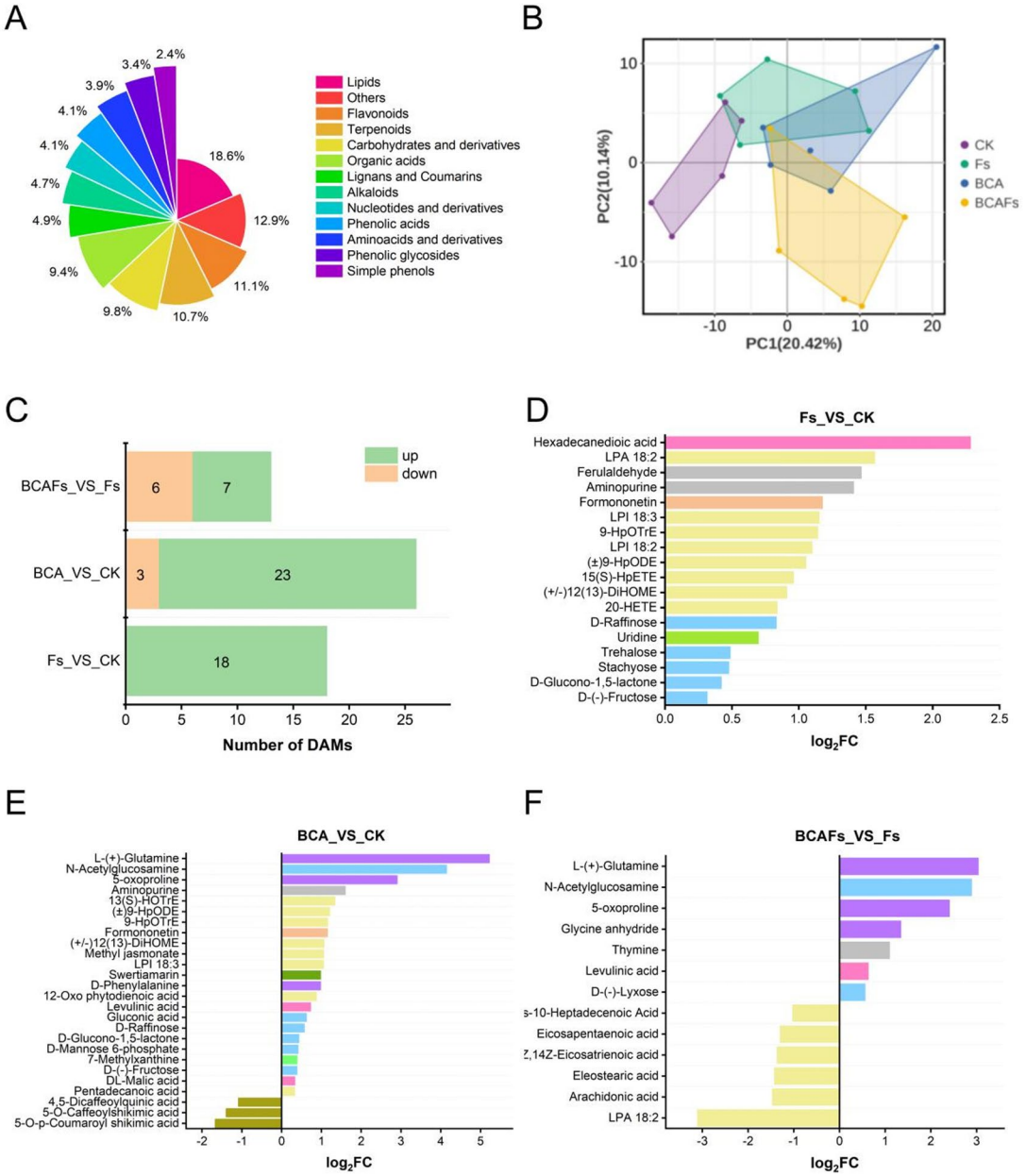

Fig. 2. Effects of the inoculation with *F. solani* and BCAs on the metabolism of *C. chinensis* root. (**A**) Chemical classification of all identified metabolites. (**B**) Principal component analysis. (**C**) The numbers of DAMs. (**D**) Difference multiple analysis of differential metabolites in the comparison group of Fs and CK. (**E**) Difference multiple analysis of differential metabolites in the comparison group of BCA and CK. (**F**) Difference multiple analysis of differential metabolites in the comparison group of BCAFs and Fs.

Transcriptional-metabolic connectivity elicited by BCA inoculation

Given the central roles of nitrogen and amino acid pathways in disease mitigation, we correlated DAMs with DEGs in these modules. Integrating the transcriptomic and metabolomic datasets (Fig. 5) revealed that the relative abundances of two amino acid related compounds—L-Gln and 5-oxoproline—were significantly correlated with the transcript levels of seven differentially regulated genes: one *NRT2*, one *NR*, three *GDH*, one *GLT1*, and one *NiR*. These metabolites and their cognate genes therefore represent potential hub components of the nitrogen and amino acid metabolism circuitry that modulates the progression of *C. chinensis* root rot.

Effect of exogenous glutamine on *F. solani* growth

Building on these results, we assessed the effect of exogenous Gln on *F. solani* colony growth on PDA plates. After 3 d of incubation, colony diameters at all five Gln concentrations did not differ significantly from the control (CK; Fig. 6, Supplementary Table S6; $P > 0.05$). By day 7, however, the 3.0 mmol/L Gln yielded a significantly

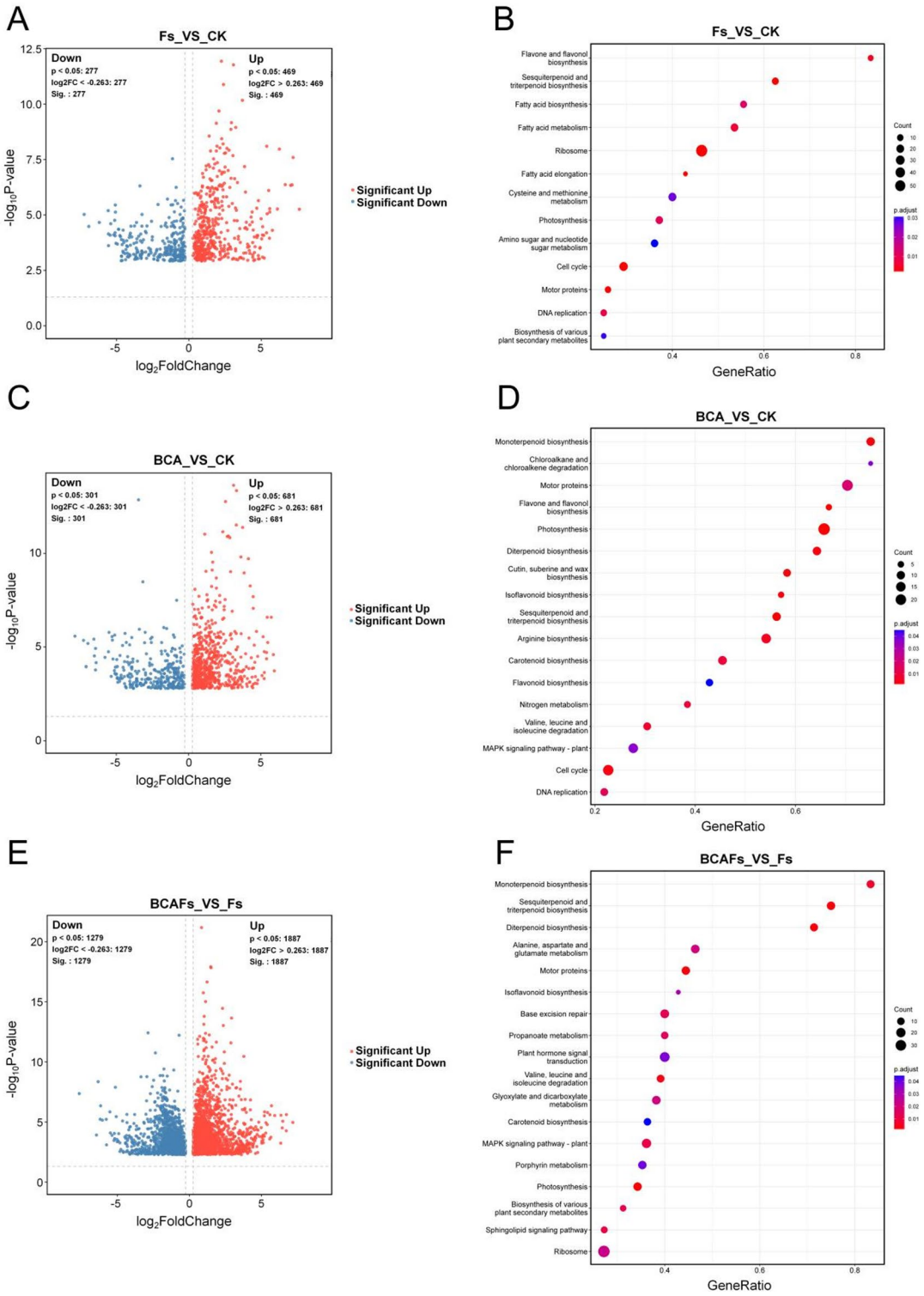

Fig. 3. Profile of DEGs in *C. chinensis* responsive to *F. solani* and BCAs colonization. (**A**) Volcano plot of DEGs in Fs vs. CK group. (**B**) DEGs enriched in KEGG pathway in Fs vs. CK group. (**C**) Volcano plot of DEGs in BCA vs. CK group. (**D**) DEGs enriched in KEGG pathway in BCA vs. CK group. (**E**) Volcano plot of DEGs in BCAFs vs. Fs group. (**F**) DEGs enriched in KEGG pathway in BCAFs vs. Fs.

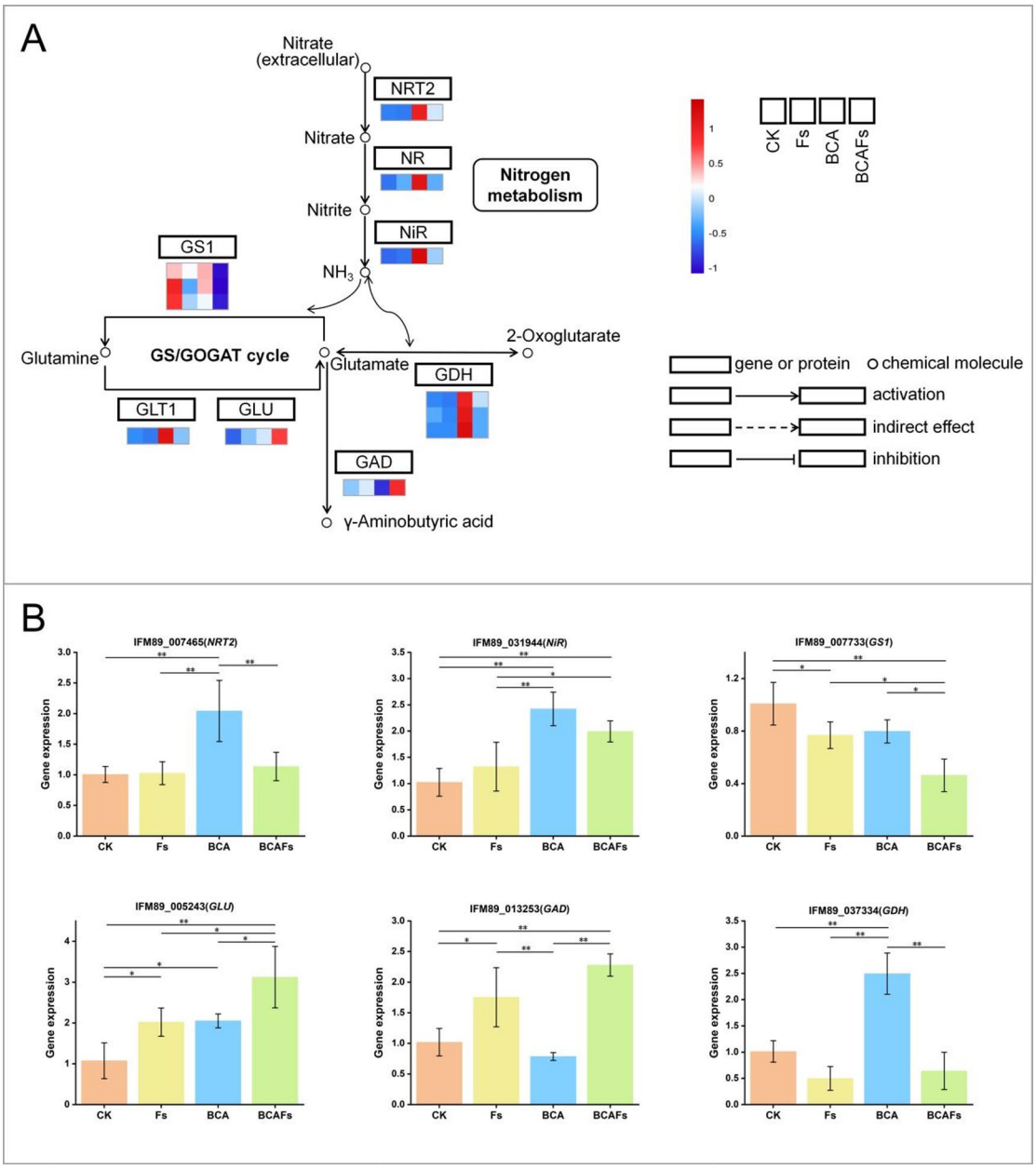

Fig. 4. The expression of DEGs is involved in amino acid metabolism and nitrogen metabolism. (**A**) Amino acid metabolism and nitrogen metabolism signaling pathway. (**B**) The transcription levels of amino acid and nitrogen related genes analyzed using qRT-PCR. Values are presented as the means ± SD of three independent replicates. $^{*}P < 0.05$, $^{**}P < 0.01$.

smaller colony than CK ($P < 0.05$), and higher concentrations produced progressively stronger inhibition, indicating a concentration-dependent effect.

Discussion

BCAs confer protective effects against *C. chinensis* root rot

Previous work showed that co-inoculation of *F. solani* with *Bacillus* spp. on detached *C. chinensis* roots reduced disease severity[28]. In the present field study, mild symptoms appeared 7 d after *F. solani* inoculation, whereas pre-inoculation with BCAs 7 d earlier partially alleviated root-rot symptoms, indicating that BCAs can likewise exert protective effects under field conditions. It should be noted that the disease index in the *F. solani*-challenged group remained relatively low (6.67%), this low initial disease severity may be attributed to the inherent environmental buffering and the specific phenological stage of the field-grown plants. Although the short duration and early infection stage meant that a statistically significant reduction in disease was not yet observable, the pronounced transcriptomic and metabolomic reprogramming of *C. chinensis* following BCA treatment clearly underscores a robust induction of host defense mechanisms. By capturing these initial

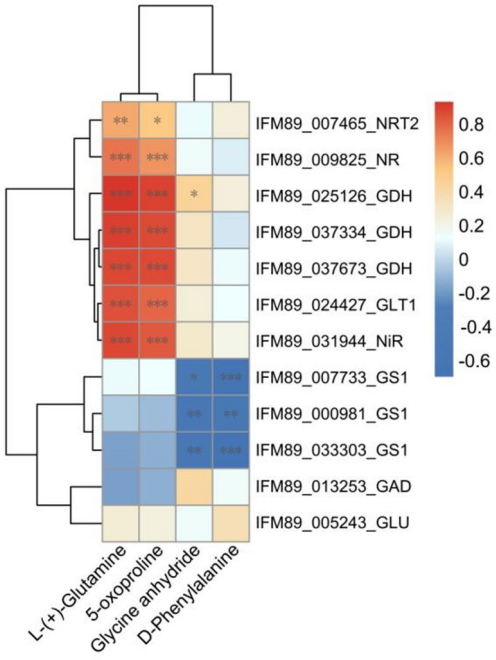

Fig. 5. The putative regulatory relationship of key metabolisms in BCA-alleviated root rot development in *C. chinensis*. Pearson's correlation analysis; asterisks indicate significance: $^{*}P < 0.05$, $^{**}P < 0.01$, $^{***}P < 0.001$.

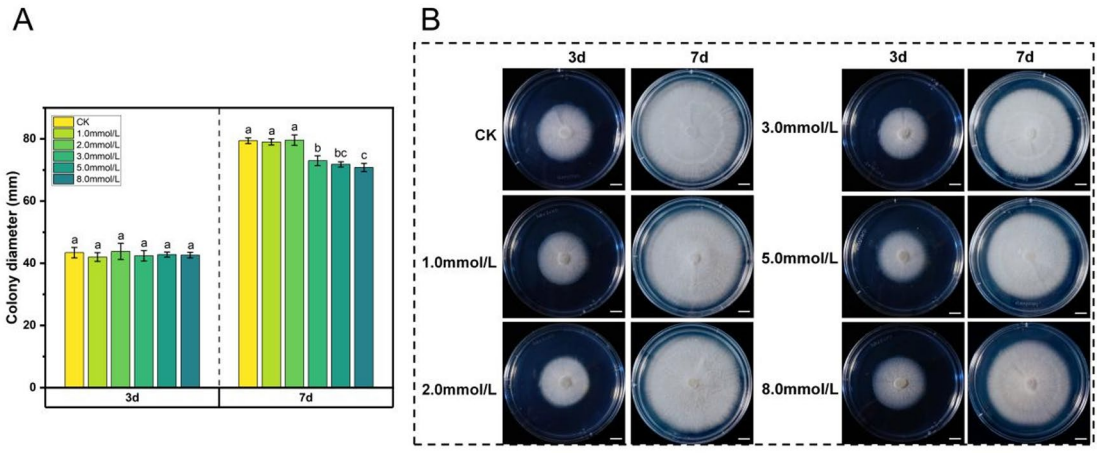

Fig. 6. Effects of Gln on the growth of *F. solani*. (**A**) Colony diameter. (**B**) Colony growth. Different lowercase letters on the bar indicated significant difference ($P < 0.05$).

molecular shifts before severe disease progression, our study provides a clearer view of the "priming" effect that characterizes early biocontrol interactions.

The four *Bacillus* strains used in this study belong to species that are well-documented for their plant-growth-promoting potential. Specifically, members of these taxa have been shown to suppress pathogens, induce systemic resistance, and produce beneficial metabolites such as IAA[42–44]. Consistent with these traits, no disease symptoms were observed in plants receiving BCAs alone during the 14-day period. Taken together, our results suggest that BCAs have significant potential for managing *C. chinensis* root rot. However, as the current mechanistic insights are derived from a single field-based time point, further research utilizing controlled pot experiments with multi-time-point dynamic monitoring is essential. Such longitudinal studies will be crucial to fully characterize the colonization patterns of the BCA consortium and its sustained regulatory effects on the host plant, thereby providing a more comprehensive and reliable evaluation of their long-term biocontrol value.

Positive roles of BCA-induced Gln accumulation in *C. chinensis* defense

In this study, BCA inoculation significantly increased Gln levels together with the up-regulation of related genes. To evaluate the biological relevance of this metabolite, we supplemented *F. solani* culture medium with

exogenous Gln; Gln significantly suppressed fungal growth in a concentration-dependent manner. However, the magnitude of this direct in vitro inhibition was relatively modest (e.g., a reduction from ~80 mm to ~70 mm at 8.0 mM). This suggests that while Gln possesses inherent antifungal properties, its direct antagonism alone may not fully account for the biocontrol efficacy. Importantly, the accumulation of Gln is likely only one component of a broader, synergistic defense response induced by the BCA consortium. Prior work similarly shows that glutamate (Glu) inhibits multiple phytopathogens[45]. Consistent with these observations, Gln can also restrain pathogen proliferation and virulence: exogenous Gln markedly limits *Magnaporthe oryzae* growth and inhibits appressorium formation[41]. In the cotton-wilt pathogen *F. oxysporum* f. sp. *vasinfectum*, among the amino acids tested, Gln and Glu selectively inhibit the naphthoquinone polyketides bikaverin (a nonaketide) and nectriafurone (a heptaketide)[46]. Moreover, exogenous Gln has been shown to suppress bacterial virulence and growth while bypassing MAMP perception and SA signaling[47]. Because Gln and Glu are coupled through the GS/GOGAT cycle- cytosolic Gln synthetase (*GS1*) assimilates ammonium into Glu to form Gln, which is then converted back to Glu by glutamate synthase[27]. Given their tight coupling, future work should disentangle their respective contributions to *C. chinensis* resistance.

Beyond direct antifungal effects, Gln likely contributes to energy provisioning, as the GS/GOGAT cycle is central to primary nitrogen metabolism and connects to the TCA cycle[27]. Adequate nitrogen supplies essential building blocks for resisting or recovering from damage, where nitrogen deficiency weakens plants and increases pathogen susceptibility[48]. Many antimicrobial proteins are nitrogen-rich (e.g., PR proteins). Overexpression of chitinase genes enhances resistance to phytopathogens in rice and lily[49,50], and chitinase activity depends on N availability[51,52]. In tomato, *PR4* expression is repressed under N limitation and induced under N sufficiency, correlating with resistance to *Botrytis cinerea*[53]. Multiple amino acids feed the TCA cycle as α-ketoglutarate, acetyl-CoA, and succinyl-CoA, supplying substrates for respiration during the energy-intensive defense response[54].

Our data align with this framework: BCA inoculation up-regulated *NRT2*, *NR*, *NiR*, *GS1*, *GLT1*, and *GDH*, indicating activation of primary N assimilation, thereby facilitating nitrogen accumulation. Following subsequent *F. solani* challenge, *GLU* and *GAD*-annotated genes were induced, indicating diversion from Gln to Glu and then to γ-aminobutyric acid (GABA). In tomato ABA-deficient mutants, activation of the GS/GOGAT cycle and the GABA shunt sustains TCA intermediates, maintaining the viability of cells surrounding *B. cinerea* lesions and ultimately strengthening resistance[55]. Collectively, these findings support a model in which BCA pre-inoculation primes the host by accelerating N assimilation and pre-accumulating C–N skeletons and ATP, eenabling a rapid and effective defense upon pathogen attack. Consistent with this model, recent studies show that exogenous Glu alone can reprogram C–N metabolism and induce the accumulation of pathogenesis-related proteins, thereby markedly suppressing microbial pathogens[56,57]. These observations underscore the need to define, mechanistically, how *Bacillus*-triggered Gln accumulation rewires C–N metabolism to confer disease resistance in *C. chinensis*.

Pre-inoculation with BCAs primes defense responses in *C. chinensis*

Upon microbial attack, plants typically activate two tiers of innate immunity: PAMP-triggered immunity (PTI) and effector-triggered immunity (ETI)[58]. In this study, the BCAFs treatment exhibited strong up-regulation of multiple genes within the MAPK and plant-pathogen interaction pathways (Supplementary Fig. S4A), eliciting a more robust defense response than inoculation with either *F. solani* or BCAs alone. Pathogens can deploy effectors to suppress PTI and establish infection, whereas beneficial microbes may transiently and locally attenuate PTI to avoid self-targeting and to establish mutualism[59,60]. In compatible interactions, *Fusarium* can suppress host defenses to facilitate intimate colonization[61], which may explain the relatively weak responses observed with *F. solani* alone. In contrast, colonization by beneficial microbes can shift plants into a primed physiological state, enabling faster and stronger responses to subsequent attack[62].

Consistent with this paradigm, in olive, neither *F. solani* Fso14 nor *Trichoderma harzianum* Ths97 alone markedly altered the expression of many immune-related genes (oxidative-stress responses, phenylpropanoid pathway, PR proteins, and JA/Et-SA hormonal status), whereas co-inoculation significantly up-regulated multiple defense genes[63]. Similarly, we observed enhanced expression of ET-, JA-, and SA-pathway components (e.g., *ERF1*, *PDF1.2*, *MYC2*, *TGA*, *PR1*) in BCAFs plants (Supplementary Fig. S4B). Systemic acquired resistance (SAR) is canonically mediated by SA, whereas induced systemic resistance (ISR) is predominantly governed by JA and ET[62]. Together, these phytohormones constitute a core signaling network that coordinates plant defense against biotic stress by engaging key nodes of the induced-resistance circuitry[64]. Although SA- and JA-dependent signaling have traditionally been viewed as mutually antagonistic[65], accumulating evidence indicates that beneficial microbes can simultaneously activate both pathways, resulting in cooperative engagement of SAR and ISR[66].

Our data support a model in which pre-inoculation with BCAs establishes a root-localized primed state in *C. chinensis* that, upon challenge with *F. solani*, activates multiple defense-signaling cascades. Notably, this molecular priming did not translate into a statistically significant reduction in the disease index in our field experiments. Since ISR is known for its broad-spectrum protective potential, future work will focus on further evaluating BCA-based immune induction and dissecting the physiology of the *Coptis–Fusarium–Bacillus* tripartite interaction.

Conclusion

This study highlights the potential of a *Bacillus*-based consortium for managing *F. solani*-induced root rot in *C. chinensis*. Our results demonstrate that BCAs contribute to disease suppression, in part by inducing the accumulation of Gln, which exhibits a direct inhibitory effect on *F. solani* growth under in vitro conditions. This pre-accumulation of Gln following BCA treatment may potentially serve as a metabolic resource to support host

defense demands. Furthermore, the BCA consortium appears to act as an immune primer that, upon subsequent *F. solani* challenge, markedly activates PR proteins and the JA, SA, and ET signaling pathways. While these findings provide initial mechanistic evidence, we must acknowledge that the observed reduction in the Disease Index did not reach statistical significance in this field trial. Therefore, further research is required to evaluate alternative inoculation strategies—including optimized dosages, application sites, and specific phenological timings—to enhance the robustness and efficacy of BCA-mediated control across diverse environments, while also more precisely delineating the underlying regulatory networks involved.

Data availability

The raw sequence data reported in this paper have been deposited in the Genome Sequence Archive (Genomics, Proteomics & Bioinformatics 2025) in National Genomics Data Center, China National Center for Bioinformation / Beijing Institute of Genomics, Chinese Academy of Sciences (GSA: CRA033710) that are publicly accessible at https://ngdc.cncb.ac.cn/gsa.

Received: 18 November 2025; Accepted: 17 April 2026
Published online: 24 April 2026

References

1. He, Y. et al. Complete Chloroplast Genome Sequence of Coptis chinensis Franch. and Its Evolutionary History. *BioMed. Res. Int.* **7** (2017). https://doi.org/10.1155/2017/8201836 (2017).
2. Xiang, K. L. et al. The First Comprehensive Phylogeny of *Coptis* (Ranunculaceae) and Its Implications for Character Evolution and Classification. *PLoS One*. **11**, e0153127. https://doi.org/10.1371/journal.pone.0153127 (2016).
3. Wang, J., Wang, L., Lou, G. H., Zeng, H. R. & Yang, X. B. Coptidis Rhizoma: a comprehensive review of its traditional uses, botany, phytochemistry, pharmacology and toxicology. *Pharm. Biol.* **57**, 193–225. https://doi.org/10.1080/13880209.2019.1577466 (2019).
4. Li, Y., Guan, S., Liu, C., Chen, X. & Li, M. Neuroprotective effects of *Coptis chinensis* Franch polysaccharide on amyloid-beta (Aβ)-induced toxicity in a transgenic Caenorhabditis elegans model of Alzheimer's disease (AD). *Int. J. Biol. Macromol.* **113**, 991–995. https://doi.org/10.1016/j.ijbiomac.2018.03.035 (2018).
5. Kong, D. et al. Research on Export Current Situation and Countermeasure of *Coptis chinensis* from Shizhu County. *Mod. Chin. Med.* **15**, 701–703. https://doi.org/10.13313/j.issn.1673-4890.2013.08.012 (2013).
6. Ke, W. et al. Relatively high light inhibits reserves degradation in the *Coptis chinensis* rhizome during the leaf expansion by changing the source-sink relationship. *Front. Plant. Sci.* **14**, 14. https://doi.org/10.3389/fpls.2023.1225895 (2023).
7. Li, J., Fan, G. & He, Y. Predicting the current and future distribution of three *Coptis* herbs in China under climate change conditions, using the MaxEnt model and chemical analysis. *Sci. Total Environ.* **698**, 134141. https://doi.org/10.1016/j.scitotenv.2019.134141 (2020).
8. Mei, P. Y., Song, X. H., Zhu, Z. Y. & Li, L. Y. First Report of Root Rot Caused by *Fusarium avenaceum* on *Coptis chinensis* in Chongqing, China. *Plant. Dis.* **105**, 1. https://doi.org/10.1094/PDIS-05-20-1110-PDN (2021).
9. Bodah, E. Root Rot Diseases in Plants: A Review of Common Causal Agents and Management Strategies. *Agric. Res. Technol.* **5**, 56–63. https://doi.org/10.19080/ARTOAJ.2017.05.555661 (2017).
10. Han, Y. et al. Root rot in medicinal plants: a review of extensive research progress. *Front. Plant. Sci.* **15**, 1504370. https://doi.org/10.3389/fpls.2024.1504370 (2025).
11. Miao, Z. Q., Li, S. D., Liu, X. Z., Chen, Y. J. & Zhang, K. Q. The causal microorganisms of *Panax notoginseng* root rot disease. *Sci. Agric. Sin*. **39**, 1371–1378. https://doi.org/10.3321/j.issn:0578-1752.2006.07.011 (2006).
12. Sun, W. S., Zhang, T. J., Liu, K. & Shen, B. Y. First Report of Root Rot Caused by *Fusarium commune* on American Ginseng (*Panax quinquefolium*) in China. *Plant. Dis.* **107**, 1. https://doi.org/10.1094/PDIS-10-21-2347-PDN (2023).
13. Rodriguez, P. A., Rothballer, M., Chowdhury, S. P., Nussbaumer, T. & Falter-Braun, P. Systems Biology of Plant-Microbiome Interactions. *Mol. Plant.* **12**, 804–821. https://doi.org/10.1016/j.molp.2019.05.006 (2019).
14. Zhang, Z. K. et al. Isolation and identification of antagonistic bacteria of *Angelica* root rot and their mechanism as biological control. *Biol. Control.* **177**, 15. https://doi.org/10.1016/j.biocontrol.2022.105120 (2023).
15. Foroud, N. A., Chatterton, S., Reid, L. M., Turkington, T. K. & Tittlemier, S. A. *Fusarium Diseases of Canadian Grain Crops: Impact and Disease Management Strategies. Future challenges in crop protection against fungal pathogens* (Springer, 2014).
16. Tagele, S. B., Kim, S. W., Lee, H. G. & Lee, Y. S. Potential of Novel Sequence Type of *Burkholderia cenocepacia* for Biological Control of Root Rot of Maize (*Zea mays* L.) Caused by *Fusarium temperatum*. *Int. J. Mol. Sci.* **20**, 18. https://doi.org/10.3390/ijms20051005 (2019).
17. Afzal, I., Shinwari, Z. K., Sikandar, S. & Shahzad, S. Plant Beneficial Endophytic Bacteria: Mechanisms, Diversity, Host Range and Genetic Determinants. *Microbiol. Res.* **221**, 36–49. https://doi.org/10.1016/j.micres.2019.02.001 (2019).
18. Carrión, V. J. et al. Pathogen-induced activation of disease-suppressive functions in the endophytic root microbiome. *Science* 606–612. https://doi.org/10.1126/SCIENCE.AAW9285 (2019).
19. Lin, L. et al. Lysobacter enzymogenes: A fully armed biocontrol warrior. *J. Integr. Agr.* **24**, 23–35. https://doi.org/10.1016/j.jia.2024.02.021 (2025).
20. Liu, Y. et al. Nonpathogenic *Pseudomonas syringae* derivatives and its metabolites trigger the plant cry for help response to assemble disease suppressing and growth promoting rhizomicrobiome. *Nat. Commun.* **15** https://doi.org/10.1038/s41467-024-46254-3 (1907).
21. Zamioudis, C. & Pieterse, C. M. J. Modulation of host immunity by beneficial microbes. *Mol. Plant-Microbe Interact.* **2**, 139–150. https://doi.org/10.1094/mpmi-06-11-0179 (2012).
22. Erb, M. & Kliebenstein, D. J. Plant Secondary Metabolites as Defenses, Regulators, and Primary Metabolites: The Blurred Functional Trichotomy. *Plant physiol.* **184**, 39–52. https://doi.org/10.1104/pp.20.00433 (2020).
23. Zaynab, M. et al. Role of secondary metabolites in plant defense against pathogens. *Microb. pathog.* **124**, 198–202. https://doi.org/10.1016/j.micpath.2018.08.034 (2018).
24. Rojas, C. M., Senthil-Kumar, M., Tzin, V. & Mysore, K. S. Regulation of primary plant metabolism during plant-pathogen interactions and its contribution to plant defense. *Front. Plant. Sci.* **5**, 17. https://doi.org/10.3389/fpls.2014.00017 (2014).
25. Meyer, T. et al. The plant defense signal galactinol is specifically used as a nutrient by the bacterial pathogen *Agrobacterium fabrum*. *J. Biol. Chem.* **293**, 7930–7941. https://doi.org/10.1074/jbc.RA118.001856 (2018).
26. Stuttmann, J. et al. Perturbation of *Arabidopsis* Amino Acid Metabolism Causes Incompatibility with the Adapted Biotrophic Pathogen *Hyaloperonospora arabidopsidis*. *Plant. Cell.* **23**, 2788–2803. https://doi.org/10.1105/tpc.111.087684 (2011).
27. Qiu, X. M., Sun, Y. Y., Ye, X. Y. & Li, Z. G. Signaling Role of Glutamate in Plants. *Front. Plant. Sci.* **10**, 1743. https://doi.org/10.3389/fpls.2019.01743 (2019).

28. Liao, H., Huang, L., Li, N., Ke, W. & Ma, Y. Auxiliary rapid identification of pathogenic and antagonistic microorganisms associated with *Coptis chinensis* root rot by high-throughput sequencing. *Sci. Rep.* **11**, 11141. https://doi.org/10.1038/s41598-021-90489-9 (2021).
29. Mooijman, K. A., Pielaat, A. & Kuijpers, A. F. A. Validation of EN ISO 6579-1 - Microbiology of the food chain - Horizontal method for the detection, enumeration and serotyping of *Salmonella* - Part 1 detection of *Salmonella* spp. *Int. J. Food Microbiol.* **288**, 3–12. https://doi.org/10.1016/j.ijfoodmicro.2018.03.022 (2018).
30. Liu, C. et al. Research Progress on continuous cropping obstacle of *Coptis chinensis*. *Heilongjiang Agric. Sci.* **10**, 102–107. https://doi.org/10.11942/j.issn1002-2767.2024.10.0102 (2024).
31. Marsell, A. & Fröschel, C. Inoculation strategies to infect plant roots with soil-borne microorganisms. *J. Vis. Exp.* **181**, e63446. https://doi.org/10.3791/63446 (2022).
32. Zhang, Y. Z. et al. Investigation and analysis of related factors of powdery mildew in *Coptis chinensis* in Chongqing. *J. Plant. Healthc.* **32**, 12–16. https://doi.org/10.13718/j.cnki.zwys.2019.02.003 (2019).
33. Cao, Z., Xia, W., Zhang, X., Yuan, H. & Gao, L. Hepatotoxicity of nutmeg: A pilot study based on metabolomics. *Biomed. Pharmacother.* **131**, 110780. https://doi.org/10.1016/j.biopha.2020.110780 (2020).
34. Gao, Y., Zhang, G., Jiang, S. & Liu, Y. X. Wekemo Bioincloud: A user-friendly platform for meta-omics data analyses. *iMeta* **3**, e175. https://doi.org/10.1002/imt2.175 (2024).
35. Mortazavi, A. et al. Mapping and quantifying mammalian transcriptomes by RNA-Seq. *Nat. Methods.* **5**, 621–628. https://doi.org/10.1038/nmeth.1226 (2008).
36. Liu, Y. et al. Analysis of the *Coptis chinensis* genome reveals the diversification of protoberberine-type alkaloids. *Nat. Commun.* **12**, 3276. https://doi.org/10.1038/s41467-021-23611-0 (2021).
37. Yang, L., Smyth, G. K. & Wei, S. featureCounts: an efficient general purpose program for assigning sequence reads to genomic features. *Bioinformatics* **53**, 923–930. https://doi.org/10.1093/bioinformatics/btt656 (2014).
38. Love, M. I., Huber, W. & Anders, S. Moderated estimation of fold change and dispersion for RNA-seq data with DESeq2. *Genome Biol.* **15** https://doi.org/10.1186/s13059-014-0550-8 (2014).
39. Minoru, K., Yoko, S., Masayuki, K., Miho, F. & Mao, T. KEGG as a reference resource for gene and protein annotation. *Nucleic Acids Res.* **D457-D462** https://doi.org/10.1093/nar/gkv1070 (2016).
40. Kanehisa & Goto. KEGG: kyoto encyclopedia of genes and genomes. *Nucleic Acids Res.* **28**, 27–30. https://doi.org/10.1093/nar/27.1.29 (2000).
41. Chen, H. F. et al. Effects of six metabolites on rice resistance to blast fungus, *Magnaporthe oryzae*. *J. South. Agric.* **53**, 57–67. https://doi.org/10.3969/j.issn.2095-1191.2022.01.007 (2022).
42. Tariq, H., Subramanian, S., Geitmann, A. & Smith, D. L. *Bacillus* and *Paenibacillus* as plant growth-promoting bacteria in soybean and cannabis. *Front. Plant. Sci.* **16**, 1529859. https://doi.org/10.3389/fpls.2025.1529859 (2025).
43. Ali, B. et al. *Bacillus mycoides* PM35 Reinforces Photosynthetic Efficiency, Antioxidant Defense, Expression of Stress-Responsive Genes, and Ameliorates the Effects of Salinity Stress in Maize. *LIFE-BASEL* **12**, 25 https://doi.org/10.3390/life12020219 (2022).
44. Bilal, B., Siddiq, Z., Iftikhar, T. & Hayyat, M. U. Mitigating NaCl stress in *Vigna radiata* L. cultivars using *Bacillus pseudomycoides*. *PeerJ* **12**, e17465. https://doi.org/10.7717/peerj.17465 (2024).
45. Yang, S., Zheng, Y., Guo, Y., Yang, Z. & Dong, Y. Faba bean–wheat intercropping and appropriate nitrogen supply control *fusarium* wilt in faba bean via altering specific amino acids in the root exudate of faba bean. *Physiol. Mol. Plant. P.* **124**, 101961. https://doi.org/10.1016/j.pmpp.2023.101961 (2023).
46. Bell, A. A. et al. United States Department of Agriculture-Agricultural Research Service studies on polyketide toxins of *Fusarium oxysporum* f sp *vasinfectum*: potential targets for disease control. *Pest Manag Sci.* **59**, 736–747. https://doi.org/10.1002/ps.713 (2003).
47. Zhang, X. M. et al. Elicitor-induced plant immunity relies on amino acids accumulation to delay the onset of bacterial virulence. *Plant. Physiol.* **192**, 601–615. https://doi.org/10.1093/plphys/kiad048 (2023).
48. Snoeijers, S. S., Pérez-García, A., Joosten, M. H. A. J. & Wit, P. J. G. M. D. The Effect of Nitrogen on Disease Development and Gene Expression in Bacterial and Fungal Plant Pathogens. *Eur. J. Plant. Pathol.* **106**, 493–506. https://doi.org/10.1023/A:1008720704105 (2000).
49. Zhang, C., Huang, M., Sang, X., Li, P. & He, G. Association between sheath blight resistance and chitinase activity in transgenic rice plants expressing *McCHIT1* from bitter melon. *Transgenic Res.* **28**, 381–390. https://doi.org/10.1007/s11248-019-00158-x (2019).
50. Francisco, F. et al. Conferred resistance to *Botrytis cinerea* in *Lilium* by overexpression of the *RCH10* chitinase gene. *Plant. Cell. Rep.* **34**, 1201–1209. https://doi.org/10.1007/s00299-015-1778-9 (2015).
51. Maglovski, M. et al. Nutrition supply affects the activity of pathogenesis-related beta-1,3-glucanases and chitinases in wheat. *Plant. Growth Regul.* **81**, 443–453. https://doi.org/10.1007/s10725-016-0222-7 (2017).
52. Dietrich, R., Plo, K. & Heil, M. Constitutive and induced resistance to pathogens in *Arabidopsis thaliana* depends on nitrogen supply. *Plant. Cell. Environ.* **27**, 896–906. https://doi.org/10.1111/j.1365-3040.2004.01195.x (2004).
53. Vega, A. et al. Transcriptome analysis reveals regulatory networks underlying differential susceptibility to *Botrytis cinerea* in response to nitrogen availability in *Solanum lycopersicum*. *Front. Plant. Sci.* **6**, 911. https://doi.org/10.3389/fpls.2015.00911 (2015).
54. Bolton, M. D. Primary Metabolism and Plant Defense—Fuel for the Fire. *Mol. plant. microbe In.* **22**, 487. https://doi.org/10.1094/MPMI-22-5-0487 (2009).
55. Seifi, H. S. et al. Concurrent overactivation of the cytosolic glutamine synthetase and the GABA shunt in the ABA-deficient sitiens mutant of tomato leads to resistance against *Botrytis cinerea*. *New. Phytol.* **199**, 490–504. https://doi.org/10.1111/nph.12283 (2013).
56. Yang, J., Sun, C., Fu, D. & Yu, T. Test for l-glutamate inhibition of growth of *Alternaria alternata* by inducing resistance in tomato fruit. *Food Chem.* **230**, 145–153. https://doi.org/10.1016/j.foodchem.2017.03.033 (2017).
57. Jin, L., Cai, Y., Sun, C., Huang, Y. & Yu, T. Exogenous l-glutamate treatment could induce resistance against *Penicillium expansum* in pear fruit by activating defense-related proteins and amino acids metabolism. *Postharvest Biol. Tec.* **150**, 148–157. https://doi.org/10.1016/j.postharvbio.2018.11.009 (2019).
58. Jones, J. D. G. & Dangl, J. L. The plant immune system. *Nature* **444**, 323–329. https://doi.org/10.1038/nature05286 (2006).
59. Yu, T. Y., Sun, M. K. & Liang, L. K. Receptors in the Induction of the Plant Innate Immunity. *Mol. Plant. Microbe Interact.* **34**, 587–601. https://doi.org/10.1094/MPMI-07-20-0173-CR (2021).
60. Yu, Y. et al. Induced Systemic Resistance for Improving Plant Immunity by Beneficial Microbes. *Plants* **11** https://doi.org/10.3390/plants11030386 (2022).
61. Alba, J. M., Glas, J. J., Schimmel, B. C. J. & Kant, M. R. Avoidance and suppression of plant defenses by herbivores and pathogens. *J. Plant. Interact.* **6**, 221–227. https://doi.org/10.1080/17429145.2010.551670 (2011).
62. Conrath, U. et al. Priming: Getting ready for battle. *Mol Plant. Microbe Interact In.* **19**, 1062–1071. https://doi.org/10.1094/MPMI-19-1062 (2006).
63. Amira, M. B. et al. Beneficial effect of *Trichoderma harzianum* strain Ths97 in biocontrolling *Fusarium solani* causal agent of root rot disease in olive trees. *Biol. Control.* **110**, 70–78. https://doi.org/10.1016/j.biocontrol.2017.04.008 (2017).
64. Van Loon, L. C., Rep, M. & Pieterse, C. M. J. Significance of inducible defense-related proteins in infected plants. *Annu. rev. phytopathol.* **44**, 135–162. https://doi.org/10.1146/annurev.phyto.44.070505.143425 (2006).
65. Li, N., Han, X., Feng, D., Yuan, D. & Huang, L. J. Signaling Crosstalk between Salicylic Acid and Ethylene/Jasmonate in Plant Defense: Do We Understand What They Are Whispering? *Int. J. Mol. Sci.* **20**, 671. https://doi.org/10.3390/ijms20030671 (2019).

66. Niu, D. D. et al. The plant growth-promoting rhizobacterium *Bacillus cereus* AR156 induces systemic resistance in *Arabidopsis thaliana* by simultaneously activating salicylate- and jasmonate/ethylene-dependent signaling pathways. *Mol. Plant. Microbe Interact.* **24**, 533–542. https://doi.org/10.1094/MPMI-09-10-0213 (2011).

Acknowledgements
We are grateful to all those who contributed to this study and to the funding.

Author contributions
Y.T.M., N.L, and H.L.L. carried out the design of this research work and writing this paper. N.L, H.L.L, W.J.K., and J.J.D. carried out the transcriptome and metabolome analysis of this work, and C.Z, F.F.X, and Y.X. participated in experiment management and manuscript revision. T.Z. and B.J.X. participated in the revision of the manuscript.

Funding
This work was supported by the National Natural Science Foundation of China (82474036), the Sichuan Natural Science Foundation (2024NSFSC2111), and the 2023 Central Government Transfer Payment Local Project 'Enhancing the Guarantee Capacity of Sichuan-Produced Local Traditional Chinese Medicine Resources'.

Declarations

Competing interests
The authors declare no competing interests.

Additional information
Supplementary Information The online version contains supplementary material available at https://doi.org/10.1038/s41598-026-49863-8.

Correspondence and requests for materials should be addressed to B.X., T.Z. or Y.M.